LANGMUIR

pubs.acs.org/Langmuir Article

Effects of Crude Oil Properties and Dispersant on the Microstructure and Viscosity of Seawater-in-Oil Emulsions

Diego F. Muriel and Joseph Katz*

Cite This: *Langmuir* 2023, 39, 2043−2062 Read Online

ACCESS | Metrics & More | Article Recommendations | Supporting Information

ABSTRACT: This study examines the effects of crude oil properties and dispersant concentration (Corexit 9500) on the evolution of bulk viscosity, viscoelastic properties, and microstructure of salt water-in-crude oil emulsions. Microscopy, followed by machine-learning-based analysis, provides the size and spatial distribution of the seawater droplets. The crude oils include light Bakken, Alaskan North Slope (ANS), and Louisiana oils, and medium to heavy Platform Henry, Cold Lake, and Platform Gina oils. The light and medium oils entrain water up to 80% by volume, and the heavy oils, up to 25%. The droplet sizes and distance between them decrease with increasing viscosity, with small droplets clustering around larger ones. The Bakken- and ANS-based emulsions are unstable, but all of the emulsions evolve in time. All exhibit a non-Newtonian behavior, with the viscosity decreasing with increasing shear rate. The storage modulus is higher than the loss modulus for light oils, and vice versa for heavy oils. Trends of their nondimensional viscosity are collapsed onto two power laws as a function of the Ohnesorge number involving the properties of the original oil, and the size or distance between droplets. For light oils, the power law exponent decreases with increasing capillary number based on the rheometer shear rate and increases for heavy oils. At high shear rates, the exponents converge to the same value, 0.45, suggesting that the oil viscosity becomes the property that defines the emulsion rheology. The present findings are consistent with previously published data. Premixing the emulsions with dispersant causes separation of most of the water from the light oils, leaving only sparse droplet concentrations. In contrast, owing to slow diffusion rate, only a small fraction of the seawater is extracted from the heavy oil emulsions. Hence, the sparse light oil emulsions become Newtonian, but the heavy ones remain non-Newtonian.

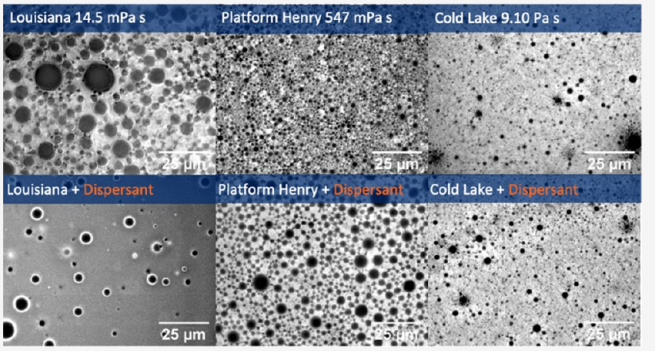

1. INTRODUCTION

Crude oil slicks resulting from oceanic spills are exposed to shear rates that fluctuate between 5 and 100 1/s under the action of breaking waves.[1,2] This process mixes the seawater with the crude oil, forming water-in-oil emulsions containing up to 80% water by volume. The emulsification increases the viscosity by up to 3 orders compared to that of the spilled crude oil and the volume of pollutants by up to 5 times.[3−6] The entrainment of water and increase in viscosity are serious obstacles to the clean-up of oil spills for several reasons, including the volume that needs to be removed, difficulties in the pumping of the very viscous fluid, challenges to in situ burning, and reduction in the efficacy of dispersants.[4,7,8] Consequently, numerous efforts have been made to develop methods for removing the water from the emulsions using, e.g., mechanical, thermal, and chemical techniques.[7,8] The common perception is that emulsification of water droplets in crude oil is enabled by the formation of interfacial films composed of naturally present asphaltenes.[9−11] The more common formation of water-in-crude oil rather than crude oil-in-water emulsions can be explained either by the Bancroft's rule or by the hydrophile−lipophile balance (HLB). The Bancroft rule[12−14] states that if an emulsifying agent is preferentially wetted by one of the phases, then more of this agent can be accommodated if the interface between fluids is convex toward that phase. Hence, the liquid in which the surfactant (asphaltene) is more soluble (oil) becomes the continuous phase, resulting in the formation of water-in-oil emulsions. Similarly, the HLB is an empirical scale that characterizes the tendency of the surfactant to preferentially dissolve in either the oil phase (low HLB) or the aqueous phase (high HLB).[15] The dominant group of the surfactant molecule preferentially orients itself to be located within the "outer phase", which for lipophilic surfactants, like resin or asphaltenes, implies the formation of water droplets in oil.[16] In contrast, oil-in-water emulsions are usually purposely designed and examples include

Received: December 4, 2022
Revised: January 13, 2023
Published: January 27, 2023

Table 1. Seawater, Dispersant, and Oil, Properties, and Emulsion Water Volume Fractions: Viscosity, μ, and Density, ρ, at 25.00 ± 0.02 °C, Interfacial Tension, σ, at 18.4 ± 0.7 °C, and Water Volume Fraction, ϕ

	fresh and weathered oils					crude oil emulsions					
	fresh			weathered		emulsified water volume fraction, ϕ (%)		water fraction extracted (±1.0%) by day 21 after premixing dispersant at dispersant-to-emulsion ratio of			
	viscosity, μ_{c_f} (mPa s)	density, ρ_{cf} (kg/m^3)	interfacial tension, σ (mN/m)	viscosity, μ_{c_w} (mPa s)	density, ρ_{c_w} (kg/m^3)	day 0	day 21	0	1/4000	1/2000	1/1000
Seawater	0.95 ± 0.01	1046.4 ± 3.6	N.A.	N.A.	N.A.	N.A.	N.A.	N.A.	N.A.	N.A.	N.A.
Dispersant	45.32 ± 0.30	977.7 ± 3.3	N.A.	N.A.	N.A.	N.A.	N.A.	N.A.	N.A.	N.A.	N.A.
Bakken	7.05 ± 0.04	873.2 ± 8.3	5.19 ± 0.13	11.98 ± 0.80	874.7 ± 50	81.3	21.1	93.9	94.6	98.4	92.3
Louisiana	8.24 ± 0.54	875.8 ± 5.8	21.55 ± 0.35	14.49 ± 0.24	905.2 ± 4.6	80.7	80.7	0	93.3	98.1	99.6
ANS	26.37 ± 0.23	924.9 ± 5.6	9.67 ± 0.31	47.82 ± 0.58	943.8 ± 11	80.5	76.6	20.5	93.3	94.6	94.1
P. Henry	151.0 ± 3.8	944.0 ± 3.7	26.95 ± 0.13	546.8 ± 27.6	960.8 ± 3.4	80.2	80.2	0	6.70	8.00	12.9
Cold lake	277.9 ± 6.3	949.8 ± 3.7	19.66 ± 0.17	9095 ± 263	992.2 ± 11	23.1	23.1	0	7.00	12.1	17.3
P. Gina	2172 ± 27.4	952.5 ± 8.6	39.98 ± 2.72	3216 ± 17.3	966.7 ± 35	25.3	25.3	0	13.1	14.5	17.7

heavy oil pipeline emulsions, oil sand flotation process slurry, and emulsion drilling fluid, among others.[17] Another common perception is that the increase in crude oil emulsion viscosity over time is associated with changes in the interfacial rigidity of the asphaltene film.[18−20] In contrast, in laboratory emulsions involving silicon oil, surfactants, and water, which also show an increase in viscosity, the macroscopic rheological changes have been attributed to the formation of solid-like networks of droplets that aggregate, hence resist deformation.[21−23] Furthermore, our own recent study of the structure and rheology of water-in-(light) crude oil emulsions[24] also links/correlates the emulsions' macroscopic properties, such as shear viscosity, non-Newtonian behavior, and viscoelasticity, to aggregation of the water droplets. Slow coalescence of the water droplets and the resulting decrease in the concentration of the droplet clusters reduce the emulsion's viscosity. Hence, it appears that both the interfacial rigidity presumably caused by the asphaltene and droplet clustering play a role in the stability and rheology of the emulsions. The compaction, deformation, and size changes of these droplet clusters also influence the emulsion's non-Newtonian response to varying shear rates.[25] While an imposed shear tends to aggregate droplets,[26,27] the clusters do not grow indefinitely. Beyond a critical shear rate, the destruction of clusters becomes greater than the creation of new ones, causing a decrease in the volume of the dispersed phase within the cluster and a reduction in the bulk viscosity.[28,29] Our previous work[24] also evaluates and modifies a phenomenological model[30−39] for the effects of fractal dimension and size of the aggregates as well as the shear strain rate, yield stress, and water volume fraction on the emulsion's viscosity for one of the present light oils, namely, Louisiana Oil. This model predicts the general trends of a decrease in viscosity with increasing strain rate, but at a rate that does not match with the data. A correction to this model involving modification to the relationship between volume fraction and yield stress provides an improved prediction of the emulsion viscosity.

Mixing dispersant with crude oil significantly reduces the interfacial tension between oil and water. For example, at a 4% concentration, there is a 2 orders of magnitude reduction.[2] However, access of the dispersant to the oil−water interface is impeded once emulsions are formed. Consequently, considerable attention has been paid to the impact of introducing dispersants on the interfacial rheology of water-in-crude oil emulsions.[17,40−49] If dispersants can access the interfaces, they could displace the natural surface-active material stabilizing the water droplets, hence reduce the thickness of the film, and decrease surface viscosity, therefore promoting coalescence.[50,51] Other studies have also examined the dispersants' capacity at varying concentrations to separate the emulsions either by spraying them in small-scale laboratory settings or based on field observations.[8,40,52−54] It was found that the molecular weight of the surfactants correlates with demulsification efficacy, where higher molecular weights perform better. Also, an optimal dosage can be found, which varies depending on the constituents of the dispersant, and for some of these dispersants, an overdosage produces a stable emulsion. It is commonly believed that spraying of dispersant is ineffective in breaking up aged emulsions. This ineffectiveness is associated with the dispersant's inability to reach the internal interfaces and modify the interfacial rheology.[44] The structural and rheological changes to water-in-(light) crude oil emulsion, once it is either sprayed or mixed mechanically with dispersant, have also been examined in our laboratory.[24] Results show that spraying of Corexit 9500 partially separates the water from the emulsion and generates Marangoni-driven flows. Upon forced mixing at low concentrations, the dispersant causes substantial phase separation, removing up to 99% of the water for a dispersant-to-emulsion ratio of 1/1000. The remaining emulsion contains mostly droplets in the submicron range at low concentrations. The viscosity becomes Newtonian, i.e., it no longer varies with shear rate, and its magnitude is only 14% higher than that of weathered pure crude oil and 4 times higher than that of the original fresh oil. Therefore, forced mixing with dispersants could be used for decanting light oils, like Louisiana oil. The present paper shows that this trait is not universal, e.g., it is not effective for heavy oils.

This study substantially expands the scope of the Muriel and Katz[24] study by examining the microscopic morphology, rheology, and effect of dispersant on emulsions containing crude oils of varying origins, with fresh oil viscosity spanning 3 orders of magnitude. Included are unstable, metastable, and stable emulsions. Fluorescence microscopy is used for examining the size, spatial distribution, and time evolution of the water droplets in the emulsions, and rheometry is used for measuring their viscosity. We show that trends of the drastically different droplet sizes and rheology can be collapsed onto two curves describing the relationship between light and heavy oil emulsion viscosity and dimensionless parameters, such as the Ohnesorge and Morton Numbers involving

https://doi.org/10.1021/acs.langmuir.2c03287
Langmuir 2023, 39, 2043−2062

Table 2. Nomenclature

Parameter	Description	First appearance (Section)	Parameter	Description	First appearance (Section)
Ca	capillary number	3.1	α	coefficient of the optimization for emulsions' length scale prediction	4.4
Ca_{macro}	macroscopic capillary number	3.1	$\dot{\gamma}$	shear rate	3.1
d	approximate thickness of thin oil film	4.2	$\dot{\gamma}_m$	angular velocity of the overhead mixer	4.2
D_{10}	simple (arithmetic) average diameter	2.0	η_n	coefficient of the 4-term Maxwell-model fit, where $n = 1,\cdots4$	2.1
D_{30}	volume mean diameter	2.0	λ_n	coefficient of the 4-term Maxwell-model fit where $n = 1,\cdots4$	2.1
D_{32}	Sauter mean diameter	2.0	μ	viscosity	2.0
DV0.5	volume median diameter	2.0	μ_e	emulsion viscosity	3.1
G'	storage modulus	2.1	$\bar{\mu}_e$	mean emulsion viscosity	4.2
G''	loss modulus	2.1	$\breve{\mu}_e$	emulsion viscosity at low shear	4.1
G^*	complex shear modulus	2.1	μ'	dynamic viscosity	3.4
h	spacing between rheometer parallel plates	3.1	μ^*	complex viscosity	3.4
HLB	hydrophile−lipophile balance	1.0	ρ	density	2.0
IDS	interdroplet spacing	3.2	σ	interfacial tension	2.0
k	Boltzmann constant	3.5.2	τ	diffusion time scale	3.5.2
L	represents relevant length scales	3.1	ϕ	water volume fraction	2.0
m	power law coefficient	4.2	ψ	diffusion coefficient	3.5.2
Mo	Morton number	4.2	ω	angular frequency	2.1
NND	nearest neighbor distance	3.2			
ND	number density	3.2			
Oh	Ohnesorge number	4.2			
r_a	molecular radius	3.5.2			
R_{32}	Sauter mean radius	2.0			
Re	Reynolds number	4.2			
T	absolute temperature	3.5.2			
We	Webber number	4.2			

Subscript	Description: use	First appearance (Section)	Subscript	Description: use	First appearance (Section)
c_f	fresh crude oil properties	2.0	NND	NND as length scale	4.2
c_w	weathered crude oil properties	2.0	opt	optimization	4.4
H_2O	salt water properties	4.2	pf	power fit	4.4
e	emulsion viscosity	3.3	R_{32}	R_{32} as length scale	4.2

properties of the original oil and the size or distance between droplets in the emulsion. The present findings are also consistent with previously reported emulsion viscosities and volume fractions. Furthermore, we identify distinctly different trends between the structure and viscosity of light and heavy oil emulsions, as well as the efficacy of dispersant as a decanting agent. The next section describes the methods, followed by a systematic presentation of results and a discussion comparing the present results to previous research and introducing the dimensional analysis.

2. METHODS

Since a detailed description of the methods used in the present study can be found in Muriel and Katz,[24] they are described briefly in this paper with additional information provided in the Supporting Information. The water-in-crude oil emulsions are created by mixing 1000 mL of 33 ppt artificial salt water with 250 mL of several crude oils of varying properties (see Table 1). The mixing is performed by an overhead laboratory mixer in an open container allowing for the evaporation of volatile compounds. The mixer operates at 660 rpm inside a fume hood at an ambient temperature of 22 °C for a total of 22 h. Once the mixing is stopped, the emulsion is kept at rest for 1 h before measuring the volumes of water not emulsified, the oil evaporated (or dissolved) during the mixing process, and the resulting entrained water volume fractions, ϕ, which are reported in Table 1 (see Table 2 for nomenclature). A parallel test verifies that the fraction of water that evaporates during the mixing process is negligible by repeating the procedures using the same salt water and silicone oil, which does not evaporate. For each emulsion, the tests (details follow) are performed after 2 h as well as 7, 14, and 21 days after the mixing. The only exception is the Bakken oil emulsion, for which only a fraction of the oil was emulsified, allowing fewer measurements which we opted to perform on days 0 (i.e., 2 h after mixing) and 21. Additionally, undisturbed samples have been kept for monitoring the phase separation for up to 2 years. Subsequently, to study the effects of using dispersant, Corexit 9500A (Nalco), a water- and oil-soluble surfactant used extensively during the DeepWater Horizon spill, is premixed with the (previously created) emulsions at volume fractions of 0, 1/4000, 1/2000, and 1/1000. The composition and properties of Corexit 9500A are provided in the Supporting Information. The mixing is performed at 1500 rpm for 99 s on day zero using a vortex mixer (VortexGinie2). The zero-fraction emulsion, which serves as a control, follows the same "mixing" procedure but without adding dispersant. These mixtures are undisturbed and kept at 22 ± 2 °C until testing on day 21. The fraction of water separated from the emulsion because of the dispersant is monitored and reported in Table 1. The water fraction remaining after mixing the emulsion with dispersant can be inferred from the data in Table 1 by subtracting the removed fraction from the content on day 21. It should be noted that consistent with our prior experience, the emulsion morphology and viscosity are affected by the mixing parameters and duration. Hence, one should maintain the emulsification time and energy to obtain reproducible results, as we

https://doi.org/10.1021/acs.langmuir.2c03287
Langmuir 2023, 39, 2043−2062

have demonstrated for the Louisiana oil.[24] Ten independent tests were conducted with Louisiana oil to establish reproducibility of the mixing protocol. Results showed that reducing the rotational speed of the mixer by 10% or the emulsification time by 30% will produce an emulsion with morphological and rheological properties, and stability significantly different from the emulsion presented herein.

Reflected light fluorescent microscopy using a Zeiss AxioObserver microscope is used for characterizing the morphology of the emulsions. To perform these observations, a sample of the top layer of the emulsion is placed in a 9 mm deep and 35 mm diameter dish and kept small enough such that the cover does not touch the emulsion. The images are recorded at several depths and in three different areas. The image resolution is 0.10 μm/pixel using a 63× oil immersion objective. The droplet diameter and spatial distributions are determined with a machine-learning-based pixel-wise classification method whose details are described in our previous publication[24] and described in more detail in the Supporting Information. First, semantic segmentation classifies the image pixels as either water or oil by implementing a random forest algorithm.[55] Second, instance segmentation classifies group of pixels as individual droplets using morphological opening, auto-local thresholding based on Otsu's method,[56] and distance transform watershed. Based on bootstrap analysis,[57−59] the maximum misclassification of diameter is 1.2%.

The droplet centroids and diameters obtained from segmentation are used for measuring the nearest neighbors' distance between droplets. The procedure involves finding five neighboring droplets with the smallest edge-to-edge distances from each droplet using a Matlab-based in-house code. The characteristic droplet diameters are obtained from the following equation

$$D_{[p,q]} = \left(\frac{\sum_i N_i D_i^p}{\sum_i N_i D_i^q} \right)^{1/(p-q)} \quad (1)$$

where N_i is the total number of droplets with diameters D_i, and p and q denote integers varying between zero and three. Hence, D_{10} is the average diameter, D_{30} is the volume mean diameter, and D_{32} is the Sauter mean diameter. DV0.5, referring to 50% of the water volume contained in droplets smaller than this value, is also presented as it represents the volume median diameter. Sample images of the emulsion morphology, as well as detailed statistics of the droplet size distributions, characteristic droplet diameters, and scales, are provided in the Results section.

2.1. Measuring the Oil and Emulsion Properties. The viscosity, density, and interfacial tension of six different oils and their emulsions with seawater have been measured as part of the present study. The chemical compositions of these oils are available in the literature. Included are Bakken,[60] Louisiana sweet MCR252,[61,62] Alaskan North Slope (ANS),[60,63] Platform Henry,[64] Cold Lake,[60] and Platform Gina[65] oils. Bakken, Louisiana, ANS, Platform Henry, and Gina are crude oils, while Cold Lake is a diluted bitumen.[60] All of the oils have been "freshly drawn" from barrels for emulsification. The viscosity of the crude oil has been measured at 25 °C with an MCR 302 Anton Paar rheometer using a 50 mm diameter cone-plate, with a cone angle of 1°, and a 50 mm fixed spacing. The selected 50 mm diameter provides sufficient contact area needed for satisfying the rheometer's minimum torque limit during measurements of low-viscosity oils. Since the crude oils are expected to be weathered owing to exposure to the atmosphere and water, we have also measured the properties of "weathered" oils after exposing them to air in a similar way to that occurring during the process of emulsification and subsequent testing periods. Specifically, 1.25 L of fresh oil samples are independently mixed for 22 h at 660 rpm in an open 4000 mL beaker inside a fume hood. Subsequently, the viscosity of this oil is measured using the same rheometer setting as that of the fresh oil, along with the volume lost, density, and interfacial tension. We have not tested the increase of viscosity due to dissolution in seawater since our previous results have shown that evaporation during mixing is the major cause of viscosity increase during weathering.[24] Changes in viscosity occurring during subsequent days have been very small. Each fresh and weathered oil viscosity is measured six independent times, 100 points each, while increasing the shear strain rate from 1 to 100 1/s and decreasing the duration of application of this shear rate from 10 to 1 s, both linearly. Some of the oils, namely, the lighter Bakken and Louisiana oil, exhibit Newtonian behavior, i.e., their viscosity does not vary with shear rate. For the heavier ANS, Henry, Gina, and Cold Lake oils, the Newtonian behavior persists up to shear rates of 70−80 1/s, but the viscosity decreases with increasing shear rate at higher levels. The non-Newtonian behavior of fresh heavy crudes has been reported previously and is attributed to the high asphaltenes and wax content.[66−68] Hence, in Table 1, we report the viscosity obtained only for the Newtonian range. The ratio of the shear stress to the shear strain rate for several strain rates in this range is least-square fitted to obtain the average value. The viscosity of the salt water is measured with a Cannon-Frenske viscometer. The oil density is measured by weighing a known volume. The oil−salt water interfacial tension, also presented in Table 1, is measured using the pendant drop method.[69,70] The uncertainty reported in this table is estimated from the 95% confidence interval of a t-distribution obtained from 10,000 randomly selected subsets of the respective set of tests. They include between 6 and 10 repetitions for viscosity and density measurements, and between 10 and 14 repetitions for interfacial tension. The viscosity of the emulsions, which is provided in the Results section, is measured with the above-mentioned rheometer using a 25 mm diameter parallel plate and a 1.0 mm gap. Switching to parallel plates with relatively large gaps is needed for maintaining a gap-to-droplet ratio exceeding 5. This plate diameter provides sufficient area to satisfy the rheometer's lower torque limit. For each test, the shear rate increases from 0.01 to 1000 1/s and the duration of application of this shear decreases from 100 to 1 s, both logarithmically. Ten data points are measured per decade, and six independent tests are completed for each emulsion age and dispersant concentration. The uncertainty is also estimated based on the 95% confidence interval of a bootstrap analysis. For two cases, namely, Cold Lake and Gina oils, we have measured the viscoelastic properties of emulsions created using the same mixing protocol as the rest of the samples shortly after mixing and 8 days later. These oscillatory measurements to determine the storage, G', and loss modulus, G'', have also been performed using 25 mm parallel plates with a 1 mm gap. Data for Louisiana oil is available from earlier tests.[24] Since fresh Henry oil is no longer available, its emulsion properties have been tested using older emulsions mixed 2.8 years earlier. Preliminary evaluation of data has shown that the linear viscoelastic condition is satisfied at an oscillation angle amplitude of 1% of a full rotation, hence it has been chosen for all of the present cases. During these tests, the angular frequency, ω, is varied from 100 to 0.1 rad/s, decreasing logarithmically. The storage and loss moduli are derived from the complex shear modulus, G^* (ratio of shear stress to shear strain), and the phase shift between shear strain and stress. In the earlier tests of Louisiana oil emulsions properties, we compared the results to predictions of several models. Results showed that only a four-parameter Maxwell's model[37] fits predicted the measured trends. Hence, we also compare the present data to this model, which is given by

$$G' = \sum_n \frac{\eta_n \lambda_n \omega^2}{1 + \lambda_n^2 \omega^2}, \quad G'' = \sum_n \frac{\eta_n \omega}{1 + \lambda_n^2 \omega^2} \quad (2)$$

where n varies from 1 to 4, and η_n and λ_n are obtained by least-square fits to the measured values of G' and G''.

3. RESULTS AND DISCUSSION

3.1. Effect of Shearing on Water Content and Viscosity. The non-Newtonian behavior of the Louisiana-based emulsion,[24] which has been linked to clustering, is also evinced in all of the presently investigated emulsions. For example, the viscosity for the Gina oil-based emulsion, μ_e, normalized by weathered, μ_{c_w}, and fresh, μ_{c_f}, crude oil viscosities, as a function of sear rate is presented in Figure

https://doi.org/10.1021/acs.langmuir.2c03287
Langmuir 2023, 39, 2043−2062

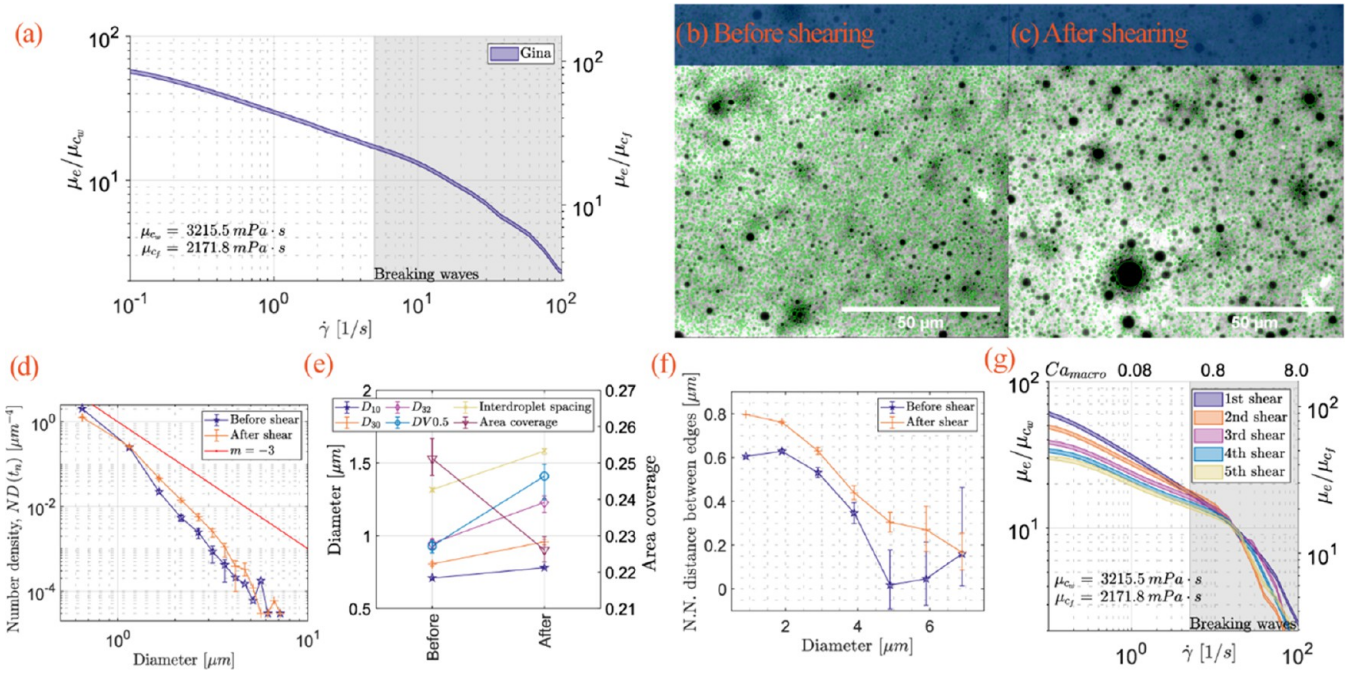

Figure 1. Effect of shear on microscopic morphology and viscosity for Gina-based emulsion: (a) viscosity as a function of shear rate; (b, c) microscopic slices before and after shearing, respectively; (d, e) statistics on the number density and length scales, respectively; (f) edge-to-edge nearest neighbor distance between droplets before and after shearing; and (g) the effect of subsequent shearing cycles on the viscosity of the same emulsion.

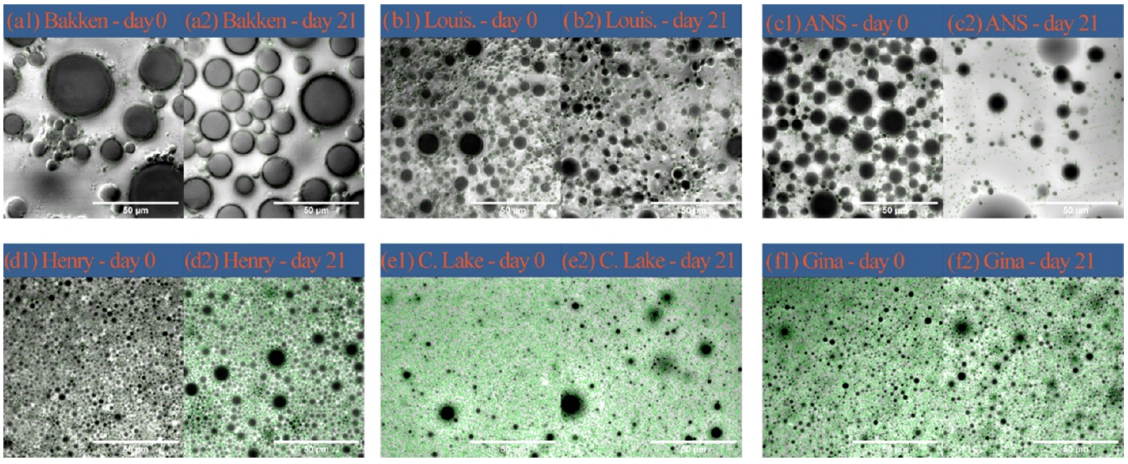

Figure 2. Microscopic slices of water-in-crude oil emulsions on day 0 and day 21. The first (a–c) and second (d–f) rows correspond to light and heavy oils (Cold Lake is a diluted bitumen), respectively. The circumference of the segmented droplet has been superimposed in green color on the original image.

1a. Here and in all subsequent viscosity plots, the shear rate range that is comparable to that of breaking sea waves is highlighted (>5 1/s)[1] and the thickness of the line represents the upper and lower uncertainty limits. The effects of applying the varying shear on the microscopic structure of this emulsion, previously unknown, are summarized in Figure 1b–g. Figure 1b,c compares sample images of the microscopic structure before and after applying shear, respectively. Oil appears bright due to its broadband fluorescence in these microscopic images, while water droplets appear black. Also, the circumference of the segmented droplet is highlighted by coloring the corresponding pixel green. They demonstrate that the shear increases the characteristic water droplets' diameter. In addition, once the top plate of the rheometer is removed, large (1 mm) water droplets appear on top of the emulsion, indicating that part of the water coalesces and separates from the bulk emulsion matrix. Quantitatively, the number density distribution (Figure 1d) shows the shearing of the sample increases in micron-sized droplets at the expense of submicron droplets coalescence. Figure 1e indeed shows that shearing increases all of the characteristic diameters and decreases area coverage. The edge-to-edge nearest neighbor distance plotted for varying water droplet diameter also increases, indicating disaggregation (Figure 1f). The effect of subjecting the same sample to repeated shearing cycles, presented in Figure 1g, shows that with the increasing number of tests, the viscosity keeps on decreasing, suggesting that the loss of water and disaggregation persists. The shear rates are expressed in a

https://doi.org/10.1021/acs.langmuir.2c03287
Langmuir 2023, 39, 2043−2062